Induced synchronization of a mobile agent network by phase locking

Lei Wang*
Laboratory of Mathematics, Information and Behavior of the Ministry of Education, School of Mathematics and Systems Science, Beihang University, Beijing 100191, China

Huan Shi and You-xian Sun
State Key Laboratory of Industrial Control Technology, Zhejiang University, Hangzhou 310027, China
(Received 17 June 2010; revised manuscript received 21 September 2010; published 25 October 2010)

We investigate synchronization issues of a set of mobile agents in plane, where each agent carries an identical chaotic oscillator and interacts with its neighbors through a blinking coupling mechanism. We discuss the effect of blinking pattern on synchronization of the related network. In particular, we show that phase locking of the blinking behavior can dramatically enhance synchronizability of the mobile agent network, while the random blinking pattern works little. Also, we show that by assessing the convergence time, the mobile agent networks with different blinking periods and duty ratios share a common idle duration which is independent of both the blinking period and the corresponding duty ratio.

DOI: 10.1103/PhysRevE.82.046222 PACS number(s): 05.45.Xt, 89.75.Fb, 89.75.Hc

The past decade has witnessed an avalanche of investigations of large-scale systems from the viewpoint of network [1–3]. Complex networks—collections of dynamical nodes connected by a wiring of edges exhibiting complex topological properties—serve as a prominent candidate to study the collective dynamics in various fields of science and engineering [3]. As a ubiquitous collective behavior, synchronization is one of the important issues that have been extensively addressed. A volume of work has demonstrated that connection topology plays a key role in synchronization of complex networks [3–6]. Thereafter, great effort has been devoted to seeking ways to enhance or optimize network synchronization, e.g., coupling-pattern regulation by strengthening the hub nodes' influence [7,8], structural modification by dividing hub nodes [9], shortening the average distance [10], deleting or adding edges [11–13], etc. Despite the extensive literatures found, most investigations have been focused on static networks, the topological structures of which do not change as time evolves. However, the constant connection topology is very restrictive and only reflects a few ideal situations. Numerous real-world networks such as biological, communication, social, and epidemiological networks generally evolve with time-varying topological structures. A more realistic description is to characterize real systems using time-varying topology. Henceforth, researchers have devoted more and more efforts to complex networks with time-varying topologies (see, e.g., [14–21]).

One interesting topic about time varying networks is synchronization in mobile agent network, where the network usually consists of a group of interactive moving agents [22]. Due to its remarkable feature of switching topology, such an agent network model has been widely used to explore various practical problems, e.g., clock synchronization in mobile robots [23], synchronized bulk oscillations [24], and task coordination of swarming animals [25]. Following this, several modified versions of mobile agent network have been introduced to investigate the corresponding synchronization issues [26–29]. Note that the switching topologies in these presented models have all been constructed based only on the proximity of agents, with little attention to the intermittent influence capability of individuals. Actually, individual units which take on an intermittent feature in influence capability are widespread in real-world systems. For example, in fireflies blinking [30], two states that fireflies emitting rays and being in nonluminous take place by turns. Evidently, none of the fireflies can interact with a firefly in nonluminous state even though they are very close to each other. Similarly, in crickets chirping in synchrony [31,32], each cricket alternates sounding state with silence state. The acoustic response appears between neighbors during its sounding interval, while acoustic interactions disappear in silence interval. Moreover, in wireless sensor networks [33], communications among sensors rest with both the transmission state of sensors and their geographical positions. No linkages can be established when sensors are in nontransmission mode even though close proximity is admitted. All these phenomena indicate that, on the precondition of close proximity, interactions between individuals exhibit a switching and intermittency property.

Motivated by the fact above mentioned, we introduce a blinking coupling mechanism to a set of mobile agents, where each agent is assigned blinking emission power to establish an intermittent coupling relationship. Under the presented blinking coupling mechanism, we thus obtain a mobile agent network to cover intermittency feature of realistic systems that has not been revealed in previous work [15,22,26–29]. Then, a study of how blinking coupling mechanism affects the dynamics on network is of primary importance. In this paper, we attempt to investigate the interplay between the structure dynamics and the collective behavior. As will be shown in the following, synchronizability of the considered network can be greatly enhanced if phase locking of blinking emission power is achieved. Also, we discuss the effect of the blinking period and the corresponding blinking duty ratio on network synchronization. All these

*lwang@buaa.edu.cn

investigations provide an insight into the regulation of time-varying networks of coupled oscillators.

Consider a set of N identical chaotic oscillators $\mathbf{x}_i(t) \in \mathbb{R}^n, i=1,\ldots,N$, each of which is associated with a mobile agent. Every agent is depicted as a random walker moving with velocity $v_i(t)$ and direction of motion $\theta_i(t)$ in a two-dimensional space of size L with periodic boundary conditions. The velocity $v_i(t)$ is constant in module (denoted by v; in the following, assume that v is sufficiently large) and is updated in direction through the angle $\theta_i(t)$ for each time unit. Then, the positions and orientations of the agents are updated according to

$$y_i(t+\Delta t) = y_i(t) + v_i(t)\Delta t,$$

$$\theta_i(t+\Delta t) = \eta_i(t+\Delta t), \tag{1}$$

where $y_i(t)$ is the position of agent i in the plane at time t, $\eta_i(t)$, $i=1,2,\ldots,N$ are N independent random variables chosen at each time unit with uniform probability in the interval $[-\pi,\pi]$, and Δt is the time unit.

We first briefly review the power-driven mobile agent network [27,28]. For the network, all agents are assigned emission powers to establish directed connections to those of the neighboring ones. In detail, each agent is considered as a wave source,

$$P_e^i = 4\pi d^2 S^i(d), \tag{2}$$

where P_e^i is the wave emission power of agent i and $S^i(d)$ is the wave intensity at a distance d from agent i. In view of limited sensing capability, a critical wave intensity S_c is introduced for the agents. That is, for agents i and j with distance d, agent j can perceive the wave from agent i if and only if

$$S^i(d) \geq S_c. \tag{3}$$

Equation (3) indicates that there exists an interaction radius $R_i=(P_e^i/4\pi S_c)^{1/2}$ for agent i with emission power P_e^i. Directed couplings from agent i to its neighbors will be established as soon as the neighboring agents move into the interaction range of agent i. From Eq. (3), couplings between agents are solely determined by the proximity of each other.

However, in various real systems, interactions among individuals depend not only on proximity of each other but also on the intermittency of influence capability; e.g., in fireflies blinking, no signal will be received if fireflies do not emit rays [30], and in wireless sensor networks, communication cannot be constructed when sensors are in sleep mode, even though they are close to each other [33]. To characterize the intermittency feature of influence capability, we adopt a so-called blinking coupling mechanism. For specific details, each agent emits wave periodically with period T_b and duty ratio γ $(0<\gamma\leq 1)$. Without lack of generality, agent i begins with idle mode in each period, and the mode lasts for a duration of $(1-\gamma)T_b$. Then, agent i switches to emission mode in the rest time of the period. In the idle mode, agent i does not emit wave at all, thus the neighboring agents could not receive any information from agent i even though they are within the interaction radius of it. While in the emission mode, agent i emits wave with power P_e^i and directed connections from agent i will be built to the neighboring agents as soon as they move into the interaction range of agent i. For the sake of simplicity, we here consider each agent to be of the same emission power, denoted by P. The following gives a formulation of the blinking coupling mechanism:

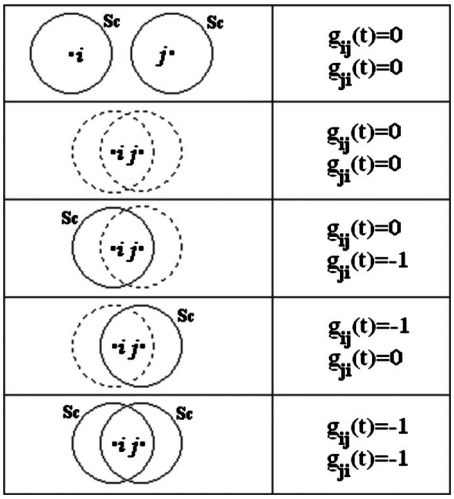

FIG. 1. Illustration of blinking coupling mechanism, where the circle denotes the neighboring range of agent, the solid lines and the dotted lines indicate an agent is in emission mode and in idle mode, respectively.

$$P_e^i = \begin{cases} P & \text{for } T_s^i + kT_b \leq t \leq T_s^i + \gamma T_b + kT_b \\ 0 & \text{otherwise,} \end{cases} \tag{4}$$

where $k=0,1,\ldots$, $i=1,\ldots,N$, and $T_s^i \in [0,T_b)$ is the instant of phase transition from idle mode to emission mode of agent i. When duty ratio $\gamma=1$, i.e., each agent of the considered network emits wave all the time, blinking coupling mechanism (4) will reduce to a special case mentioned in Refs. [27–29].

Hence, we construct a time-varying dynamical network by combining the chaotic oscillators, mobile agents, and their blinking coupling rules. The mobile agent network can be formulated as follows:

$$\dot{\mathbf{x}}_i = \mathbf{f}(\mathbf{x}_i) - \sigma \sum_{j=1}^{N} g_{ij}(t)\mathbf{h}(\mathbf{x}_j), \tag{5}$$

where $i=1,2,\ldots,N$, $\mathbf{f}:\mathbb{R}^n \to \mathbb{R}^n$ governs the local dynamics of oscillator, $\mathbf{h}:\mathbb{R}^n \to \mathbb{R}^n$ is a vectorial output function, $\sigma>0$ is the coupling strength, and Laplacian matrix $G(t)=[g_{ij}(t)] \in R^{N\times N}$ defines the coupling relationship of agents at a given time t. Note that Laplacian matrix $G(t)$ is determined not only by the trajectory of each agent but also by the blinking wave emission of each agent. Figure 1 shows an illustration of coupling relationship between two agents i and j. It is observed that, for two agents i and j, $g_{ij}(t)=-1$ [or $g_{ji}(t)=-1$] as agents i, j are neighbors and j (or i) is in emission mode; while the connection disappears if agent j (or i) is in idle mode or the distance between i and j is larger than $(P/4\pi S_c)^{1/2}$. Generally, the Laplacian $G(t)$ is asymmetric owing to different phase-transition instants T_s^i.

In the following, we conduct a series of numerical simulations to investigate the synchronous motion of network (5) under the blinking coupling mechanism. Due to the random initial conditions and the random mobility of agents, we introduce two statistical indices: synchronization error $\delta x(t) = (\sum_{i=1}^{N} \|x_i - x_1\|)/(3N)$ and synchronization index $\langle \delta x(t) \rangle$, which is averaged over 50 realizations of $\delta x(t)$ during a long enough time in the steady state, say, from T to $T+\Delta T$, to measure synchronization process of the related network. For the chaotic oscillator, without lack of generality, we consider the Rössler one, the state dynamics of which is described by $\dot{x}_{i1} = -(x_{i2} + x_{i3}), \dot{x}_{i2} = x_{i1} + a x_{i2}, \dot{x}_{i3} = b + x_{i3}(x_{i1} - c)$, with $\mathbf{x}_i = [x_{i1}, x_{i2}, x_{i2}]^T$ and $a=0.2$, $b=0.2$, $c=7.0$. Also, we choose $\mathbf{h}(\mathbf{x}^i) = H\mathbf{x}^i$, where $H = \mathrm{diag}(1,0,0)$. If not otherwise specified, the other parameters are set as $T=500$, $\Delta T=100$, $\Delta t = 10^{-3}$, and $v = 10^3$ and the initial state of each oscillator is set to $[1,1,1]^T$ with a random small deviation from it.

First, consider the case that the phase-transition instants of agents are completely in disorder, i.e., T_s^i, $i=1,2,\ldots,N$, are randomly distributed in the interval $[0, T_b)$. Then, at any moment, there are γN agents emitting waves with power P in average (generally, network order N is considered to be large enough). In particular, each possible topology of network (5) switches rapidly from one to another under the fast-switching constraint. According to Ref. [34], synchronization of network (5) can be well predicted by the average network

$$\dot{\mathbf{x}}_i = \mathbf{f}(\mathbf{x}_i) - \sigma \sum_{j=1}^{N} \bar{g}_{ij} \mathbf{h}(\mathbf{x}_j), \tag{6}$$

where $\bar{g}_{ij}$ is the element of the average Laplacian matrix $\bar{G} = \frac{1}{T}\int_t^{t+T} G(\tau) d\tau$, and time window T is a constant. Furthermore, network (5) achieves synchronization if all nonzero eigenvalues of $\bar{G}$ locate in the interval $[\alpha_1/\sigma, \alpha_2/\sigma]$, where α_1 and α_2 are constants determined by the master-stability function corresponding to network (6) [6]. By elementary transformation, we derive the N eigenvalues of $\bar{G}$: $\lambda_1 = 0$, $\lambda_2 = \cdots = \lambda_N = NP\gamma / 4 S_c L^2$. Thus, under the case of randomly distributed T_s^i, network (5) is synchronizable if power density of agents $\rho_e = NP\gamma / L^2$ lies in the bounded region $\mathcal{S} = [\rho_{e1}, \rho_{e2}]$, which is consistent with the result in Ref. [27], where $\rho_{e1} = 4 S_c \alpha_1 / \sigma$, $\rho_{e2} = 4 S_c \alpha_2 / \sigma$. Particularly, the theoretical result shows that, for the mobile agent network (5), it works little for the enhancement of network synchronization by introducing random blinking coupling mechanism.

For the case that T_s^i, $i=1,\ldots,N$ are assigned in an ordered way, i.e., $T_s^1 = \cdots = T_s^N$, network is said to achieve phase locking of blinking wave emission. It is easy to verify that under the phase locking case, the topology of network (5) is completely disconnected during the idle mode, while it satisfies fast-switching constraint in the emission mode. In other words, the whole network alternates between a fast-switching topology and a totally disconnected one. However, under the phase locking case, synchronization of network (5) cannot be investigated by applying the fast-switching constraint since the idle mode takes a relatively long duration. Figure 2 reports the comparison between the phase locking

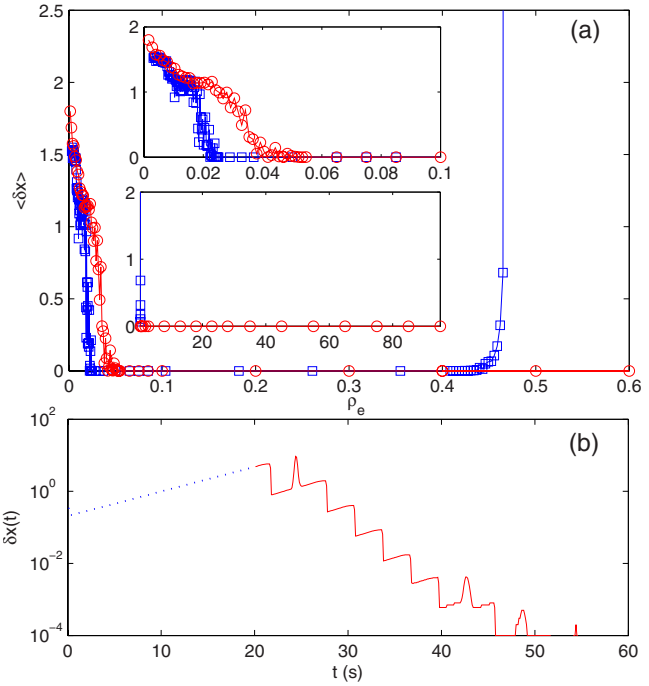

FIG. 2. (Color online) (a) Synchronization index $\langle \delta x \rangle$ vs power density ρ_e in random-phase transition case (blue square) and phase locking case (red circle), where the insets are $\langle \delta x \rangle$ as a function of ρ_e in the region [0,0.1] and [0,100], respectively. (b) Evolution of synchronization error $\delta x(t)$, where $\rho_e = 2.354 > \rho_{e2}$ keeps invariant, T_s^i, $i=1,\ldots,N$, is assigned to be randomly distributed before $t=20$ s (the dotted blue line) and to be phase locking after 20 s (the solid red line). In simulations, let $N=100$, $T_b=3.0$ s, $\gamma=50\%$, $P=3.14$, $S_c = \frac{1}{4}$, and $\sigma=10$.

case and the random T_s^i case. As expected, for randomly distributed T_s^i, the synchronization index $\langle \delta x \rangle$ presents a bounded zero-value region which corresponds to complete synchronization of network (5), while network (5) under phase locking condition can still achieve synchronization even when the power density is larger than 78.5. A power density larger than 78.5 means that the agents of network (5) are all in close proximity, and thus the topological structure alters between an all-to-all coupling one and an absolutely disconnected one. That is, the upper bound of power density disappears if phase locking is guaranteed. This result further indicates that phase locking can greatly enhance network synchronization: for a particular network [Eq. (5)] with random blinking case, the synchronization region corresponding to the power density $\mathcal{S}$ exhibits to be a bounded interval; when phase locking is guaranteed, $\mathcal{S}$ will reduce to an unbounded region. A simple verification is reported in Fig. 2(b). It has been shown in Fig. 2(b) that, during the whole process, what we do is only adjusting the phase-transition instants of the agents. Besides, the lower bound of power density corresponding to the phase locking case is a little larger than that of the random T_s^i case in Fig. 2(a), indicating that, under the phase locking case and fast-switching constraint, it is still an effective way to derive the lower bound of the power density by average network.

The above discussions are based on a particular blinking period T_b under which the idle mode takes a relatively long

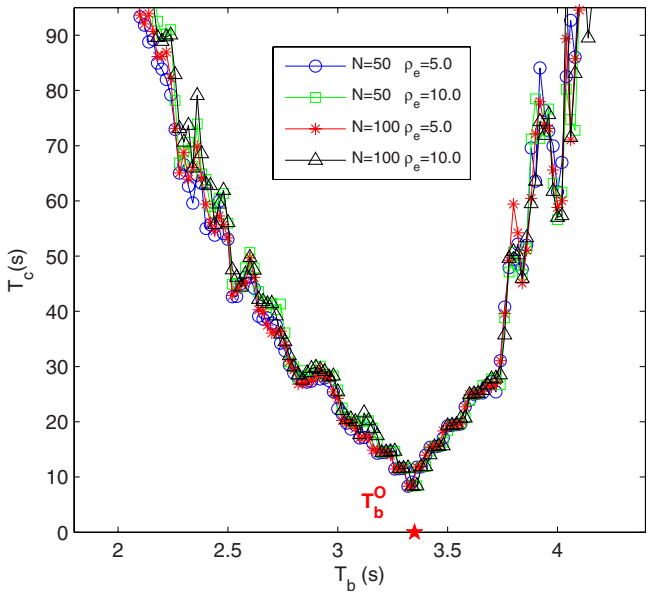

FIG. 3. (Color online) Convergence time T_c vs blinking period T_b with different agent number and power densities, where γ=50%, P=3.14, $S_c=\frac{1}{4}$, and σ=10. The optimal solution T_b^O is labeled as ⋆ in the figure.

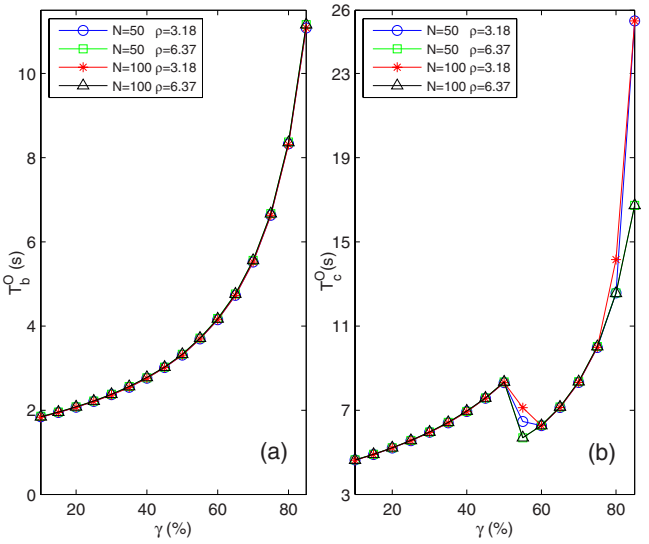

FIG. 4. (Color online) (a) Optimal blinking period T_b^O and (b) corresponding optimal convergence time T_c^O in different duty ratio γ with four combinations of agent number N and agent density ρ, where P=3.14, $S_c=\frac{1}{4}$, and σ=10.

duration. One extreme case is that the blinking period T_b is sufficiently small such that the idle mode is of very short duration. Then, no matter how T_s^i are randomly distributed or in locking state, synchronization of network (5) can be solved by applying the fast-switching constraint. Moreover, network (5) under the condition of phase locking cannot achieve synchronization if the power density is larger than the upper bound ρ_{e2}, which is quite different from the results above obtained. The other extreme case is that the blinking period T_b is long enough. Then, a long emission mode and a long idle mode will govern the topology of network (5) alternatively. During the long emission mode, network (5) with a large order also evolves as a fast-switching case, and the power density larger than upper bound ρ_{e2} leads network (5) to a nonsynchronization behavior. While in the subsequent idle mode, all agents in network (5) randomly move in plane without any interactions. Thus, synchronization of network (5) with a sufficiently long blinking period, either in phase locking case or not, is guaranteed if the power density lies in a bounded region.

From the previous analysis, the scale of blinking period T_b plays an important role in network synchronization. Either a small T_b or a large T_b is not suitable to synchronize network as the power density is beyond the upper bound ρ_{e2}. The following provides simulations to investigate how T_b influence the evolution of dynamics on network (5). Similar to Ref. [28], we introduce a performance index: convergence time T_c, which is defined as the total time from the very beginning to the instant that complete synchronization is achieved. (In simulations, $\langle \delta x \rangle \leq 10^{-4}$ means the achievement of complete synchronization.) Also, we pay attention to the power-density region lying beyond the upper bound ρ_{e2} mainly because of the contribution of phase locking to synchronization in this interval. Figure 3 shows the convergence time T_c vs the blinking period T_b with different network orders and power densities. It has been shown in Fig. 3 that the convergence time T_c behaves as a convex function of blinking period T_b. Surprisingly, no matter what network orders and power densities are, the relation between T_c and T_b can be approximately fitted by a same curve. Furthermore, there exists an identical optimal solution of T_b, denoted by T_b^O, for which T_c reaches minimum. Also observe that, when T_b is too small or too large, T_c approaches to infinity, representing the divergence of network (5).

As a matter of fact, the duty ratio γ also plays an important role in synchronizing the mobile agent network. For a given blinking period T_b, duty ratio γ determines not only the idle mode time but also the power consumption, which is a key performance index of the wireless sensor network in engineering [35]. Intuitively, a smaller duty ratio means a lower energy consumption. However, a too small value of γ is likely to cause a nonsynchronized motion. Moreover, if duty ratio γ tends to 1, i.e., there exists a sufficiently short idle mode duration. Then, no matter phase locking is achieved or not, network (5) can be assessed under the fast-switching constraint. Hence, synchronization of network (5) cannot be achieved if power density is larger than ρ_{e2}. Hereafter, we prefer the duty ratio not to be too large or too small. Figure 4 reports the optimal blinking period T_b^O and the corresponding optimal convergence time T_c^O vs duty ratio γ under different network orders and agent densities, where agent density is defined as $\rho=N/L^2$ and duty ratio γ is restricted in the interval [0.1,0.85]. From Fig. 4, the optimal solution of convergence time T_c^O can be approximately fitted by a monotonic ascending curve with regard to γ except for an abrupt change in a small γ region around [0.5,0.6]. That is, on the premise of a proper range of power density, we can choose a small duty ratio to improve the system performance. In particular, though differences exist in network order and agent density, all the four curves of T_b^O in Fig. 4(a) behave almost

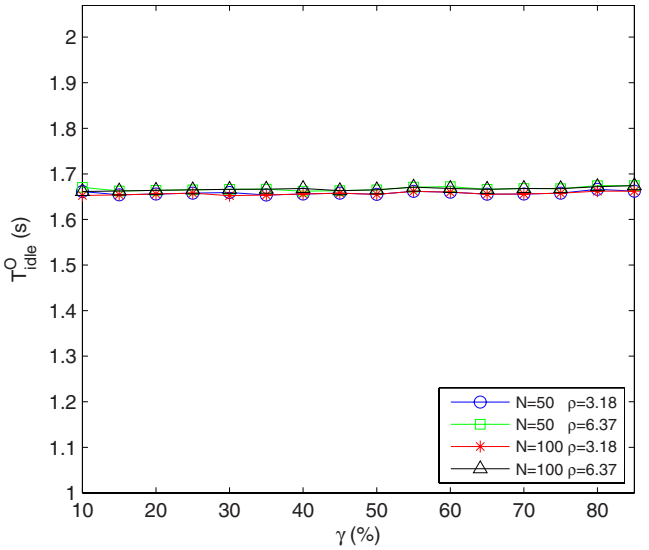

FIG. 5. (Color online) Idle mode time T^O_{idle} in optimal blinking period of different emission mode duty ratio γ in different combinations of agent number N and agent density ρ, where $P=3.14$, $S_c=\frac{1}{4}$, and $\sigma=10$.

the same, with a monotonic increase feature with respect to γ. Multiply T^O_b with $(1-\gamma)$, we get the idle mode time T^O_{idle} in the optimal situation. Figure 5 shows the numerical result of T^O_{idle} vs γ. It is found that T^O_{idle} in different duty ratios possesses the same value (about 1.67 s). There seems to exist an interesting phenomenon that T_{idle} determines the optimal performance of the whole network. To confirm this, we conduct another simulation for the optimal duty ratio γ^O in different blinking periods T_b as shown in Fig. 6. From the figure, γ^O increases with the blinking period T_b, yet the idle mode time T^O_{idle} keeps constant ($\approx$1.67 s), which further validates that the optimal idle mode time T^O_{idle} serves as an effective metric to design an optimal network.

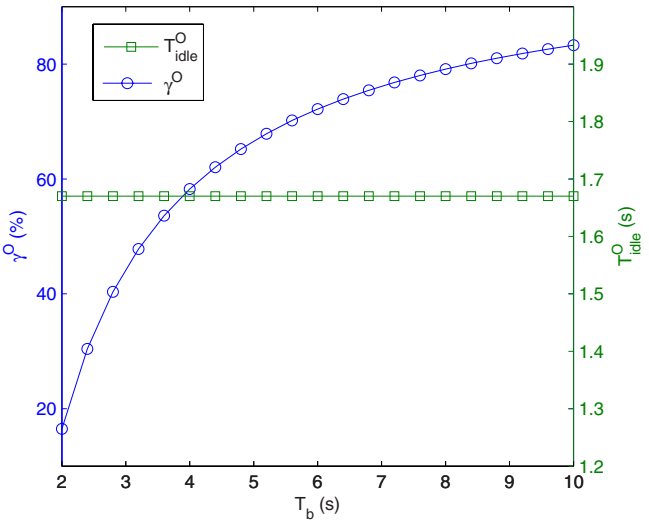

FIG. 6. (Color online) Optimal duty ratio γ^O and the corresponding idle mode time T^O_{idle} in different blinking period T_b, where $N=100$, $\rho=3.18$, $P=3.14$, $S_c=\frac{1}{4}$, and $\sigma=10$.

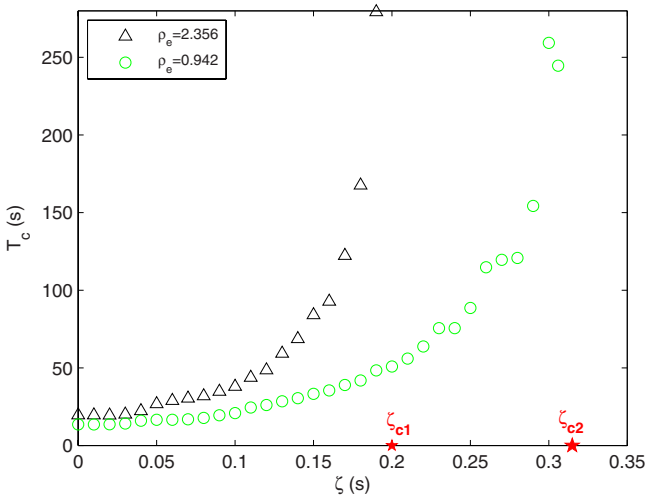

FIG. 7. (Color online) Convergence time T_c vs disorder of phase transition ζ for the case of power density beyond the upper bound ρ_{e2}, where $N=100$, $T_b=3.0$ s, $T^e_s=1.5$ s, $\gamma=50\%$, $P=3.14$, $S_c=\frac{1}{4}$, and $\sigma=10$. The critical value ζ_{c1} and ζ_{c1} are labeled as ⋆ in the figure.

There is no doubt that it is a rigorous condition for real systems to guarantee complete phase locking due to various factors such as the clock drift in wireless sensor networks [35]. We here explore the robustness against phase-transition disorder for the synchronized behavior of network (5), especially for the case of power density beyond the upper bound ρ_{e2}. A reasonable assumption is to characterize the order of blinking phase transition in a statistical way. Concretely, consider that the phase-transition instants T^i_s are distributed according to normal probability in the interval $[0,T_b)$ with expectation T^e_s and standard deviation ζ. Obviously, ζ serves as a measure of transition phase order: a large ζ means a high degree of disorder and $\zeta=0$ means the blinking emissions are in locking state. By evaluating the convergence time T_c, Fig. 7 reports the influence of ζ on network evolution, where the power density of network (5) is assigned to be larger than the upper bound ρ_{e2}. From Fig. 7, it is seen that disorder in phase transition can deteriorate the system performance. For a particular power density in Fig. 7, the convergence time T_c increases monotonically with ζ, and the slope of the curve of T_c grows rapidly as ζ evolves. Apparently, there exists a threshold value of ζ: T_c approaches infinity as ζ tends to such a threshold. Also observe from Fig. 7 that the threshold value of ζ possesses a relatively small value in the case of a relatively large power density ($\zeta_{c1}<\zeta_{c2}$). As a result, the synchronized behavior of network (5) with a larger power density is more sensitive to the order of blinking phase transition. It also reflects that the phase locking helps to synchronize network (5) when power density is larger than the upper bound ρ_{e2}. However, a counterintuitive phenomenon occurs when the power density lies between the lower bound ρ_{e1} and the upper bound ρ_{e2}. As shown in Fig. 8, the curve of T_c does not increase monotonically with ζ but behaves as a convex function of ζ. There exists an optimal solution of ζ, denoted by ζ^O, for which network (5) converges to a common orbit with a maximum speed. From Fig. 8, it can be noted that disorder in phase transition may improve system

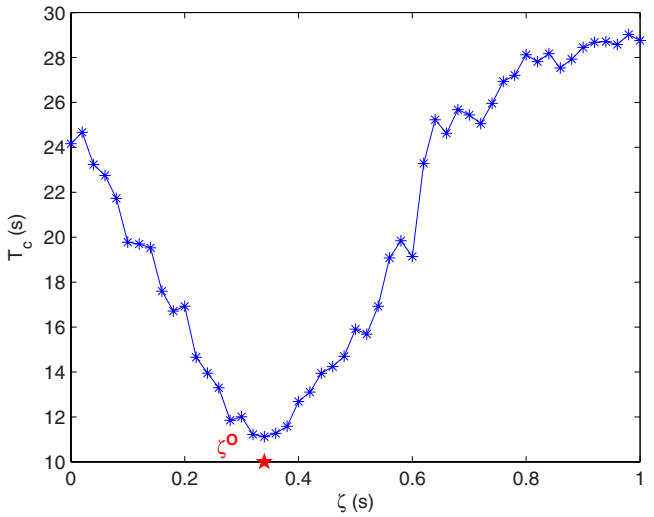

FIG. 8. (Color online) Convergence time T_c vs disorder of phase transition ζ for the case of power density between ρ_{e1} and ρ_{e2}, where $N=100$, $T_b=3.0$ s, $T_s^e=1.5$ s, $\gamma=50\%$, $P=3.14$, $\rho_e=0.219$, $S_c=\frac{1}{4}$, and $\sigma=10$. The optimal solution ζ^O is labeled as $\star$ in the figure.

performance in terms of convergence time T_c when power density is a moderate one (between ρ_{e1} and ρ_{e2}).

In conclusion, we have numerically studied synchronization of a mobile agent network with blinking emission powers, showing that the presence of blinking phase locking greatly helps enhance synchronizability of the mobile agent network. As the blinking wave emissions behave from disordered state to consensus, the region of the power density for which the considered network can be synchronized is reduced from bounded to unbounded. We have also shown that, under phase locking, the mobile agent networks with different blinking periods and duty ratios share a common idle duration by evaluating the convergence time, which provides further insights into switching topology control for synchronization of coupled complex networks.

ACKNOWLEDGMENTS

This work was supported by the Fundamental Research Funds for the Central Universities and the National Natural Science Foundation of China Grant No. 61004106.

[1] A.-L. Barabási, Science **325**, 412 (2009).
[2] S. Boccaletti, J. Kurths, G. Osipov, D. L. Valladares, and C. S. Zhou, Phys. Rep. **366**, 1 (2002).
[3] S. Boccaletti, V. Latora, Y. Moreno, M. Chavez, and D.-U. Hwang, Phys. Rep. **424**, 175 (2006).
[4] A. Arenas, A. Diaz-Guilera, J. Kurths, Y. Moreno, and C. S. Zhou, Phys. Rep. **469**, 93 (2008).
[5] G. Wen, Q. Wang, C. Lin, G. Li, and X. Han, Int. J. Bifurcation Chaos Appl. Sci. Eng. **17**, 1753 (2007).
[6] L. M. Pecora and T. L. Carroll, Phys. Rev. Lett. **80**, 2109 (1998).
[7] A. E. Motter, C. S. Zhou, and J. Kurths, Europhys. Lett. **69**, 334 (2005).
[8] A. E. Motter, C. S. Zhou, and J. Kurths, Phys. Rev. E **71**, 016116 (2005).
[9] H. Hong, B. J. Kim, M. Y. Choi, and H. Park, Phys. Rev. E **69**, 067105 (2004).
[10] T. Zhou, M. Zhao, and B. H. Wang, Phys. Rev. E **73**, 037101 (2006).
[11] C. Y. Yin, W. X. Wang, G. Chen, and B. H. Wang, Phys. Rev. E **74**, 047102 (2006).
[12] Z. Duan, G. Chen, and L. Huang, Phys. Rev. E **76**, 056103 (2007).
[13] T. Nishikawa and A. E. Motter, Proc. Natl. Acad. Sci. U.S.A. **107**, 10342 (2010).
[14] I. V. Belykh, V. N. Belykh, and M. Hasler, Physica D **195**, 188 (2004).
[15] J. D. Skufca and E. M. Bollt, Math. Biosci. Eng. **1**, 347 (2004).
[16] J. H. Lü and G. R. Chen, IEEE Trans. Autom. Control **50**, 841 (2005).
[17] M. Frasca, A. Buscarino, A. Rizzo, L. Fortuna, and S. Boccaletti, Phys. Rev. E **74**, 036110 (2006).
[18] M. Chen, Phys. Rev. E **76**, 016104 (2007).
[19] X. Q. Wu, Physica A **387**, 997 (2008).
[20] L. Wang, H. P. Dai, and Y. X. Sun, Int. J. Robust Nonlinear Control **19**, 495 (2009).
[21] S. M. Qin, G. Y. Zhang, and Y. Chen, Physica A **388**, 4893 (2009).
[22] M. Frasca, A. Buscarino, A. Rizzo, L. Fortuna, and S. Boccaletti, Phys. Rev. Lett. **100**, 044102 (2008).
[23] A. Buscarino, L. Fortuna, M. Frasca, and A. Rizzo, Chaos **16**, 015116 (2006).
[24] S. Danø, P. G. Sørensen, and F. Hynne, Nature (London) **402**, 320 (1999).
[25] L. Peng, Y. Zhao, B. Tian, J. Zhang, B. H. Wang, H. T. Zhang, and T. Zhou, Phys. Rev. E **79**, 026113 (2009).
[26] F. Peruani and G. J. Sibona, Phys. Rev. Lett. **100**, 168103 (2008).
[27] H. Shi, L. Wang, H. P. Dai, and Y. X. Sun, Physica A **389**, 3094 (2010).
[28] L. Wang, H. Shi, and Y. X. Sun, EPL **90**, 10001 (2010).
[29] L. Wang and Y. X. Sun, J. Stat. Mech.: Theory Exp. (2009), P11005.
[30] S. M. Lewis and C. K. Cratsley, Annu. Rev. Entomol. **53**, 293 (2008).
[31] T. J. Walker, Science **166**, 891 (1969).
[32] V. Nityananda and R. Balakrishnan, J. Comp. Physiol. [A] **193**, 51 (2007).
[33] J. K. Hart and K. Martinez, Earth-Sci. Rev. **78**, 177 (2006).
[34] D. J. Stilwell, E. M. Bollt, and D. G. Roberson, SIAM J. Appl. Dyn. Syst. **5**, 140 (2006).
[35] B. Sundararaman, U. Buy, and A. D. Kshemkalyani, Ad Hoc Netw. **3**, 281 (2005).